Abstract

The 2014-2015 Vandal Hybrid Racing team's mission is craft a high performance hybrid racecar that is safe, reliable and capable of competing with comparable FHSAE vehicle. The main goals for the development year are to resolve several critical issues that occurred in the previous designs presented last year. These particular issues are associated with the Brake System, Suspension, Accumulator design, and the unique Yamaha engine developed at the University of Idaho.

The next goal of the year is to create several new systems to supplement the performance that was achieved by the previous year. The critical systems that have been improved are the Tractive, Internal Combustion, Suspension and Control systems. The Tractive system has been upgraded to fully utilize the power and torque of the electric motor on the vehicle. While the Internal Combustion System has a new calibration which improves the power delivery, peak power and torque. The suspension system weight has been reduced to increase the roll stiffness of the vehicle to improve the handling of the vehicle while dropping overall weight. The Control system is improved by the use of a two dimensional look up table allowing for improved hybrid performance and fuel economy while simplifying the system.

The third and final goal for the development year is weight reduction. The vehicle in the 2013-14 competition weighed in at 561 lbs. without a full tank of gasoline. The team is attempting to bring the dry vehicle weight down to 500 lbs. This is to be achieved by the use of lighter materials and new designs that allow parts to perform multiple functions and the repackaging of several components.

Tractive System

The tractive system for the 2014-2015 vehicle uses the same components found the previous design. The electric motor is a Lynch LEM 200 D135 RAGS, the motor controller is a Kelly KDH12601E. The battery pack however features a new design to simplify and improve safety and reliability of the tractive system while using the same Haiyin lithium polymer pouch cells. The new accumulator design can be seen in Figure 1. The design of the accumulator features several unique design changes that have improved the safety, reliability and performance of the Tractive System.

The new accumulator design features a new container material to drop the manufacturing cost of the pack and allow the construction to take place in house. The design uses UHMW, a robust and fire resistant material that ensures the structural integrity of the system in the event of an accident. To keep production costs down a firewall equivalency test is conducted on the material so that the non-certified UHMW material meets or exceeds UL94-V0 flame rating. Using the non-certified UHMW brings the cost of the container down by approximately $1500. The UHMW is welded together using a Seeley 11005 plastic welder and 5/32" HMW filler rod as recommended by the manufacturing company. The overall weight of the new design has been simplified, resulting in a weight reduction of nearly 30 lbs. by using new materials and ensuring components serve multiple functions when possible.

Cell Expansion Experiment

Expansion of pouch cells is a major concern for all accumulator designs that use pouch cells and must be understood to ensure the safety and reliability of the system. To better understand what occurs during normal operation a test was conducted using single cells and a resistor bank made of nichrome wire. The cell is discharged into the nichrome wire and cell temperature, voltage, current, and expansion are simultaneously recorded in time. Figure 2 shows the experimental set up used to conduct the testing. The experimental data is logged with a USB12-bit NI-6068 data logger; temperature is recorded using a thermal couple, voltage using clamps at the terminals, current using a current clamp and expansion using a Keyence IL-1000 Laser.

The experiment is repeated for a discharge rate near 50A, 100A, 150A and 200A were multiple cells are tested to validate the results. The cell Expansion experiment shows that under the worst case scenario individual cells would only expand 13.8% and generate 20 watts of heat each. The largest expansion only occurs at a discharge of 200 amps and only occurred after 105 seconds into the experiment. The cells reached 8% expansion after 90 seconds into the tests. Figure 3 shows the results from the 200 amp test where the largest cell expansion occurred. A thermal camera is also used to determine the local hot spots that the cells developed during discharge as seen in Figure 4. The thermal image shows that during a 200 amp test the cells tabs would reach a peak temperature of 80 degrees Celsius and heat would then spread throughout the cell and become fairly distributed across the surface of the cells at around 50 degrees Celsius as shown in Figure 5.

A second test was conducted where the cells are discharged for 10 second bursts of time and then shut off for 10 seconds which is repeated until the cells reach a the shutoff voltage or temperature recommended by the manufacture. This second test shows that under a bust loading the cells do not begin to expand until after 90 seconds, and the test is terminated at 155 seconds when voltage reach the operational limit. The expansion seen during the test demonstrated an expansion of only 3.2% at the center of the cell. Figure 6 shows the data collected during the experiment.

Expansion Limiter and Thermal Management

The accumulator pack also uses 3M thermally conductive silicone padding commonly used for integrated circuits found on computer chips. The material is electrically isolating and thermally conductive. This unique combination of material properties allows the pack to use a simpler design that pulls heat away from the cells while allowing for the expansion of the pouch cells. The foam allows for 8-12% expansion while keeping pressure on the cells such that they are firmly held in place during normal operation. The expansion limiter uses two sheets of ULTEM 100O-PEI at the ends of the stack to apply a compressive load on the cells during expansion. The material is electrically isolating, and UL94V-O rated and has a tensile strength of 16.5 ksi.

To ensure that the accumulator pack would dissipate the thermal energy generated during extreme use a heat transfer model is utilized to determine the heat generation of the cells with the 3M thermally conductive padding in between individual cells. The model simulates an ambient temperature of 42.77 C and current flow of 200 amps which generates 20 watts which is data taken from the cell expansion testing. The model shows that with the 3M thermally conductive padding the cells should stabilize at a temperature of 50 C. This equilibrium temperature also assumes that the cells can

sustain a current discharge of 200 amps for an extended period of time. However given that the cells have only a 6 amp-hr capacity the cells become drained in 108 seconds at a discharge rate of 200A.

Performance Improvements

Given the information regarding the ability of the accumulator pack the tractive system is also upgraded to fully utilize the electric motor. The motor cables have been increased from 4 AWG to 1 AWG while the fusing has also been increased to 200 amps. This allows the vehicle to generate 28 HP and 31 ft-lbs for a short period of time allowing for better acceleration performance. Used properly with a control system the longevity of the system can be tuned for the duration of an event to maximize performance while maintaining the fuel economy of the vehicle.

The improvement of the design and development of the accumulator box possesses the ability to reduce electric acceleration times, weight of the system, reliability and safety. The development of the new container design cost approximately $500 for the UHMW and the tools and filler material. This is a sever reduction in production cost from the previously designed container which cost around $2700. The overall construction of the new accumulator and hardware cost a total of $2500 for the cells, container material, battery management system, and the accompanying safety equipment while reducing the overall weight of the vehicle by approximately 5%.

Internal Combustion System

The Internal Combustion engine in use in the 2014-15 vehicle is the previously designed and developed engine and a Motec M800 ECU. The engine has seen some modifications to improve the reliability and functionality of the system. The calibration of the engine is altered to create better transitions and fuel economy of the engine over the entire rpm range. The calibration also improves the cold starting ability of the engine along with stabilization of the idling point of the system. The engines cooling system is also altered to allow for better cooling efficiency and survivability of the engine.

Engine Calibration

The calibration of the engine is the largest contributor to the performance of an engine. With this fact in mind the engine is recalibrated to achieve a stable air fuel ratio using a Borghi and Saveri eddy current dynamometer. To calibrate the engine an LM2 wide band lambda sensor is used to determine the air fuel ratio of the engine in conjunction with the dynamometer. To calibrate the engine it is run at individual points with in the map and the fueling value is swept to find peak power. Spark timing is then swept until a peak power is recorded with the dynamometer. This process is repeated until the power is at a maximum for the point in the fueling and spark timing map and then again for the rest of the points with in the maps. This is done in an engine temperature range of 40 to 80 degrees Celsius to simulate normal operating conditions such that engine temperature compensations do not infringe upon the power produced by the engine.

The results of the new calibration of the engine are that the transitions from point to point are considerably smoother during engine operation. The new calibration also allowed the reduction of fuel used during operation over a wide range of operational points. During on vehicle testing the recalibration boosted fuel economy from an average of 21 to 23 mpg to 26 to 29 mpg for a range of drivers. The new calibration also yielded a peak power of 32 at 11500 and a peak torque of 18 at 8500. The power and torque curves for the new calibration compared to the stock set up in shown in Figure 7. Initial testing of the new calibration of the engine has shown that the calibration allows the engine to operate at minimum specific fuel consumption of 260 g/kW-hr. The previous calibration would at best allow the engine to achieve a specific fuel consumption of approximately 300 g/kW-hr.

Cooling System

The liquid cooling system utilized on the engine is modified from previous years to allow for a single large radiator rather than the two smaller radiators used on the stock motorcycle. The cooling system underwent this modification to allow for larger frontal area of the radiator and to reduce weight. The original layout has a frontal surface area of 0.463 ft^2 with the two smaller radiators plumbed in series and orientated parallel with the vehicle. The new design uses a surface of 0.917 ft^2 which allows for a larger cooling capacity for the engine to ensure the longevity of the system. The larger radiator allows for a drop in exit temperature of 10 C at a constant air velocity of 15 m/s. The larger radiator also makes a significant drop in the required speed to hold a constant exit temperature as shown in Figure 8.

The cooling system of the engine is undergoing several other modifications to the overflow tank, and side pods. The overflow tank serves several purposes; the first is to act as a mounting point for the radiator to limit the number of tabs required on the vehicle. The overflow tank also separates the air flow from the shear panel of the chassis and directs it over the radiator the promote heat transfer. The radiator is also modified to have a flaring on the far outside to push the air up to the side pod wall and cause a vacuum which pulls air from behind the radiator. This setup forces air through the radiator to improve the efficiency of the radiator. Figure 9 shows a rendering of the modified radiator and overflow tank on the vehicle.

To promote air flow through the radiators the side pod of the vehicle has also been modified. The side pod of the vehicle is modified to have cut outs in near the rear of the vehicle. These cut outs allow air to pass through the side pods rather than forming an air dam which increases the air resistance during vehicle operation. The flow of air though the side pods also allow for better heat transfer over the radiators, and powertrain systems such as the engine and electric motor.

Suspension System

The suspension of any vehicle is critical to the overall performance of the vehicle. With that in mind the suspension system received special attention to improve the overall performance of the vehicle. This is achieved by reducing the weight of the system with the implementation of carbon fiber a-arms and titanium uprights. The weight reduction is intended to improve the reaction time of the vehicle's suspension and thereby improving the grip of the vehicle during dynamic events. The titanium uprights are also designed to incorporate adjustable Ackerman to improve handling characteristics for different events and drivers while reducing weight. The suspension geometry is augmented as well to make the rear toe predictable by the relocation of the rear toe link. The new rear toe link geometry is also intended to ensure the minimal deflection of the link such that rear toe is maintained during bump.

Rear Geometry

The rear geometry of the suspension previously utilized on the vehicle allowed for a tight and clean package. The design however allowed the toe adjustment arm to deflect under load which gave the rear suspension unacceptable tire play under loading. The previous design can be seen in Figure 10 which shows that the

adjustment link. Given the design a considerable force could be applied to the link from the mechanical advantage due to the connection geometry. To remedy the issue the design team used Wingeo to simulate the geometry of the rear suspension and placement of a new toe link to decrease the mechanical advantage of the tire loading through the link. The design aside from minimizing the deflection of the link also minimized the bump steer the rear tire sees over its 2.25 inches of travel.

The solution to the toe link design required a new attachment point to the chassis. Given the current chassis design the rear toe link attaches to an aluminum sheet metal structure attached to the differential housing shown in Figure 11. The structure is created originally from 6061 O aluminum to allow the metal forming process to take place without cracking the material at the bend radius. The aluminum pieces are then heat treated to a T6 to achieve the desired strength. The parts are then riveted together due to the unavailability of the 4346 Aluminum filler rod. The rivets used are Cheri Max CR3213-4-2 rivets which are capable of a 664 lbf loading in single shear. The loading used in the design of the toe bracket called for the use of 102 rivets, primarily along the critical points in the structure. An FEA of the bracket with a loading of 750 lbf was simulated and calculated to have a safety factor 2.5 which is far greater than what is to be expected from normal operational parameters.

The initial design used welds to support the loading however the correct filler rod, 4346 is very difficult to come by in small quantities. The 4346 rod is heat treatable filler that allows the welding of T6 aluminum while maintaining homogeneous yield strength along the weld. Should another filler material be used sections of the welds may have lower yield strength compromising the integrity of the part in critical areas. To keep the added weight of the part at a minimum the design was changed to use rivets. The part does however have some small non critical sections welded after heat treatment to simplify the manufacturing process. The welds ensure that there is adequate rigidity to the structure under complex loading scenarios unforeseen by the initial design parameters and used in tight spaces were adequate room was unavailable for a rivet. The welded potions of the bracket are shown in Figure 12.

Carbon Fiber A-arms

In the development of the suspension system carbon fiber a-arms have been implemented to improve the performance of the vehicle. The weight reduction achieved by the use of carbon fiber allows for higher roll stiffness by the reduction of un-sprung mass. Higher roll stiffness allows the suspension to keep the tire contact patch with the ground allowing for greater traction during dynamic events.

The majority of the a-arms are made from 0.63 inch O.D. and a wall thickness of 0.065 inches. The inserts are made from 7075 T6 Aluminum which has an Ultimate tensile strength of 83 ksi. The strength of the tubes is important to the design however the bond strength of the a-arms and inserts is vastly more important. Knowing this testing is conducted on the bond strength achievable with two different kinds of epoxy, HYSAE-120HP and Hysol 9430. Table 1 shows the results of testing the bond strength of the two epoxies with an insert length of 0.5 inches. From the data shown in Table 1 the design moved forward using HYSAE-120HP given its higher bond strength over the Hysol 9430. The testing next considered the length of the inserts or bond surface. Table 2 shows the results of testing with insert lengths of 0.5, 0.75, 1 inches. From the information presented in Table 2 a sizing of the insert lengths is possible from the predicted loading on the a-arms. The final lengths and dimensions of a-arm and insert lengths along with predictive strengths of the adhesive bond and surface area prediction strength are shown in Table 3. The finished product of the construction of the a-arms is shown in Figure 13.

The designs of the a-arms have a significant safety factor indicating that the design is over built. However, even with the large safety factor the use of carbon fiber a-arms with aluminum inserts showed a weights saving of approximately 2.2 lbs. per corner on the vehicle. This weight savings tallied up yields an overall weight reduction of 8.8 lbs. while improving the capability of the vehicle.

Titanium Uprights

To further the goal of improving performance of the vehicle while reducing the overall weight of the vehicle the design utilizes a new titanium upright design. Manufacturing of titanium components can be incredibly difficult and great care must be taken when working with the material. There are various species of titanium available and considerations must be made upon the selection of the proper species. The uprights use 6AL-4V Titanium for its strength properties, heat treatability, weld properties, and wide availability.

The manufacturing process used when working with Titanium is critical to the successful implementation of the products. A fixture is used to weld the uprights which minimize the warping of the Titanium plates due to the welding. To weld the Titanium sheets a purge block is used to ensure that the weld in not contaminated while welding. After the welding is completed the finished upright is then stress relieved at 480C-595C for 4 hours and then air cooled. The material is then solution treated at 940C-970C for 10 min and then water quenched. After the solution treatment the uprights are then aged at 480-595C for 6 hours and then left to air cool. After which the uprights should have ultimate tensile strength of 170 ksi with minimal warping to parts providing a light, but strong component.

The titanium uprights are similar to the previous design with minor changes. The bearing carrier is thinner going from 0.25 inches 0.125 inches thickness to reduce the weight of the design. The mounting holes for the kingpins have doublers built into the design such that slop in the system in less lightly to occur due the bearing stress placed upon the material by the king pin yielding the surrounding material. The titanium sheet used on the uprights is thicker than previous designs but the material added is compensated for by the removal of holes along the sheet as shown in Figure 14. The front Titanium uprights shown in Figure 14 also feature an adjustable steering attachment which allows for the Ackerman of the vehicle to be tuned for different event and drivers. The Titanium uprights are approximately 2 lbs. lighter then there steel counter parts which allows for 8 lbs. savings from the overall vehicle weight.

Control System

The control system previously utilized on the vehicle functioned using a single hybrid power split in the Energy Management System which has been modified to improve performance and simplfy the system. The original Energy Management (EMS) served two distinct functions, the first to determine when to operate the vehicle with a hybrid or an internal combustion configuration. This determination enabled the system be tuned for efficiency by limiting the use of the electric system. The second function of the EMS is to split the power demand into a percentage and feed the alternative throttle demands to the respective controllers.

To improve performance and fuel economy and to create a more robust system the pervious control system saw improvements for the 2014-15 development year. The system is to incorporate a two dimensional look up table containing the power split percentage

values. These values similar to the previous design are then sent to the respective controllers utilized in the powertrain system. This new design is intended to allow the control system to have a greater effect on the fuel economy of the vehicle over a wider range of operational parameters. The new system also features a conditional statement that limits the output of the values in the lookup table based upon the State of Charge (SOC) of the Accumulator pack to improve the fuel economy of the electrical system. Figure 15 shows the new control system flow diagram.

The control system is designed to function from a minimum number of input signals. The system bases the power split percentage from the ground speed of the vehicle and the throttle demand from the driver. Ground speed is a control axis because it is independent of the gear ratio of the transmission which would require a gear detection system and further complicate the system while adding little functionality. Using the ground speed also allows for a simple calculation to help determine when the electric motor should be limited due to efficiency.

As part of the upgrade, the control system platform is moved to the Hercules micro-controller. The Hercules features 32-bit ARM Cortex-R4 central processing units running in a lock step and a built in self-test. The use of the Hercules allows for increased security of the control system particularly where the throttle signals are concerned for safety concerns.

Aerodynamic Diffuser

The diffuser design was optimized using CFD techniques and the final design was tested with a scale model in University of Idaho's wind tunnel and the results were compared to the 3D CFD results. Advanced surfacing techniques were employed to create a design that was curvature continuous. Simulation and experimental results show a significant improvement in the coefficient of lift, from nearly zero to -0.8. In addition, there is a negligible increase in the coefficient of drag

Initial simulations created for the diffuser featured a fixed rake diffuser design in a 2D CFD model. The simulations considered 4, 9, 15, 30 degree rakes along with simulations without a diffuser. The results of the simulations are for comparative purposes and not actual drag coefficients are shown in Table 4. The results shown in Table 4 clearly demonstrate that the 9 degree rake outperformed the other angles considered using the drag to lift ratio as a scale. However from Figure 16 an observable amount of turbulence is generated at the onset of the diffuser rake making a fix rake design undesirable.

To address the turbulence generation a diffuser is simulated with a curvature continuous B-spline. Four distinct B-splines are simulated to determine if the turbulence generation can be reduced. Table 5 shows the results of the B-spline diffuser simulations which are collected for comparative purposes. From Table 5 it is clear that curve 2 shows the most promising results. Curve 2 is used as the blue print for the basic diffuser shape.

Using curve 2 a diffuser was designed and modeled and is shown in Figure 17. A model diffuser is then printed and tested in the wind tunnel with a model of the vehicle shown in Figure 18. The model was tested at several speeds to determine the full effect of the diffuser upon the vehicle. To supplement the results of the experimental model a 3D CFD simulation was created. The results of the experimental study and simulation are shown in Table 6 from which we see that the two methods are, within reason, similar. The total predicted down force that the diffuser can achieve versus speed of the vehicle speed is shown in Figure 19. From Figure 19 the max force that the simulations predict the diffuser is capable of is 100 lbs. due to the vehicle top speed limitation of 65 mph.

Brake System

The Brake system is one of the most critical systems featured on a vehicle given its inherent purpose. The system features the same system developed previously with in house built master cylinders and a movable peddle assembly to accommodate different drivers. The system is slightly redesigned to resolve an issue that arose in the previous competition and to reduce the weight of the system particularly the un-sprung mass.

The master cylinders are redesigned to resolve the seizing issue which occurred in the previous year. The seizing of the calipers to the rotors occurred due to the thermal expansion of the brake fluid during normal operation. In a typical brake system when the brakes are not in use there is a clear path from the calipers to the reservoir. This path allows the fluid to freely expand from heat buildup. The previous design of the master cylinders did not allow for this clear path to exist under normal operation. To resolve this issue the design of the master cylinders is changed to have a positive stop on the check valve to ensure that it is normally open when the brakes are not in use. Figure 20 shows the new design with the positive stop. This small design change resolved the issues with brake seizure and allows the system to function as intended.

The rotors of the brake system are improved to reduce the un-sprung mass of the system as well as reduce the thermal stress induced upon the rotors during normal operation. The new design features four fully floating rotors made from A-2 steel, with an aluminum inner rotor to say weight. Figure 21 shows new front designs which are very similar to the rear rotor design. The new designs use less A-2 the previous designs and the change of geometry of the cut outs has reduced stress concentrations. The front rotors removed 0.25 lbs. from the front um-sprung mass and the rear rotors removed 0.6 lbs. from the rear.

Summary

In summary the 2014-2015 has been a successful year seeing many new designs and processes emerge. The year has seen to the redesign of several key systems to redress issues, to improve the reliability and performance of the vehicle. Several systems have also seen enhancements that enable the vehicle to achieve a higher level of performance. Through the redesign of several of the systems the vehicle has also seen significant weight reduction from the previous year. The vehicle design has lost approximately 11% weight through diligent work and innovative design solutions. The breakdown of the weight reduction of the design is presented in Table 7, which shows a total of 61.9 lbs. difference from the previous year. The table also shows that 32% of the weight removed is from the un-sprung mass of the vehicle.

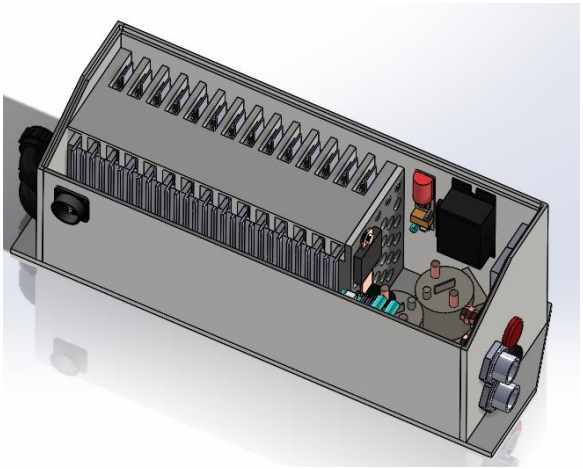

Figure 1 Accumulator Design Render

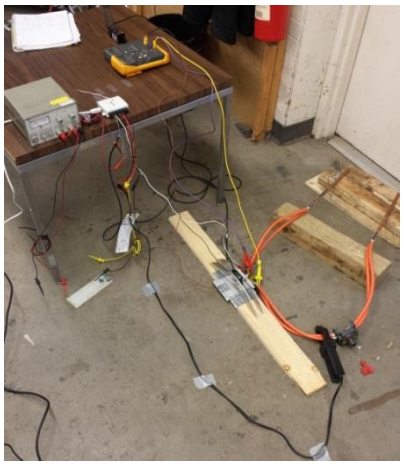

Figure 2 Cell Expansion Test Bed

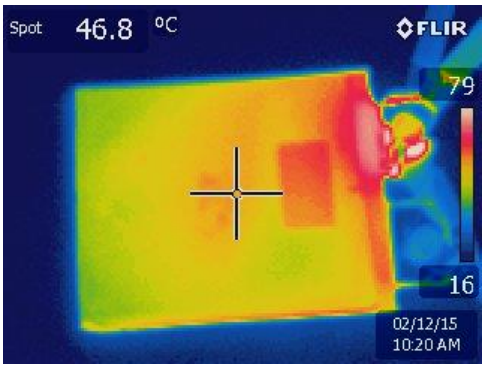

Figure 4 Thermal Image of Cell (Initial)

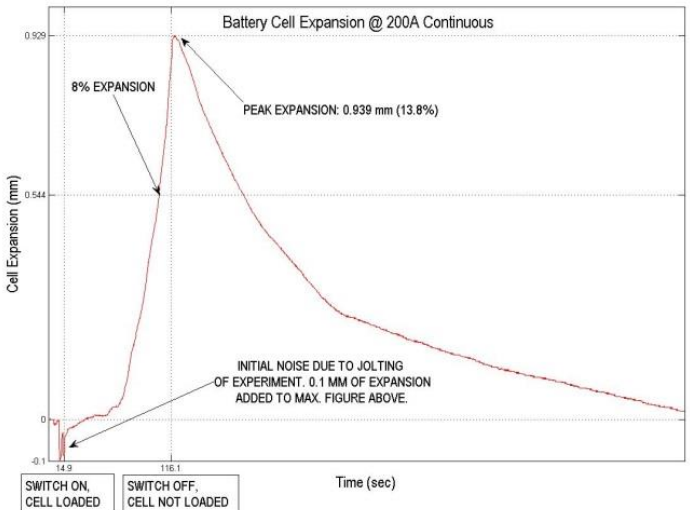

Figure 3 200 Amp Expansion Data

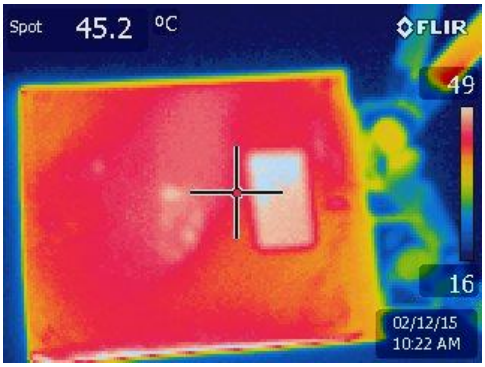

Figure 5 Thermal Image of Cell (final)

Figure 14 Titanium Upright Render

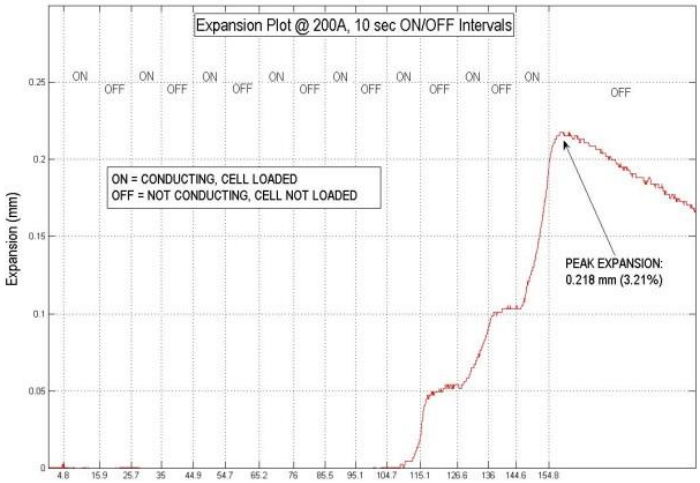

Figure 6 Digital Expansion Cell Test 200 Amps

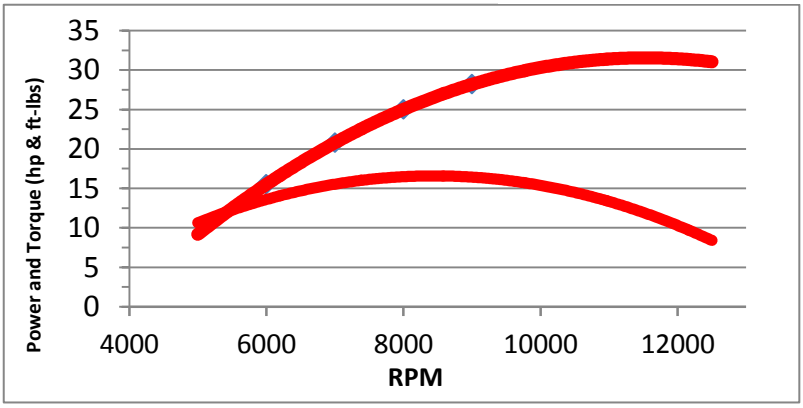

Figure 7 Power and Torque Curves

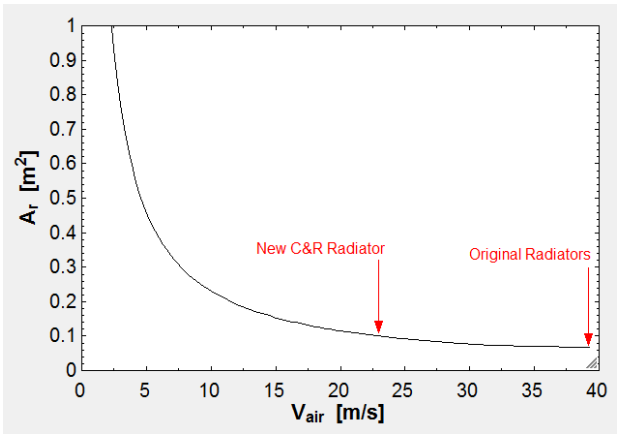

Figure 8 Frontal Area Vs. Velocity at Constant Temperature

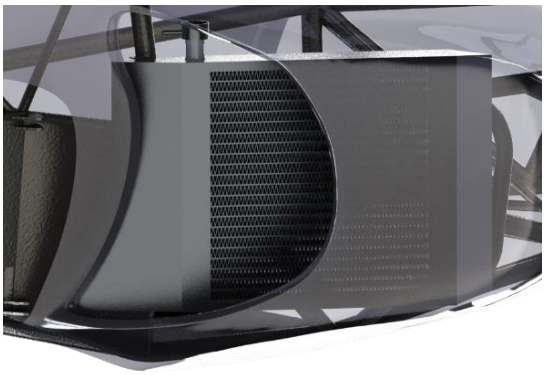

Figure 9 Modified Side Pod w/ Radiator

Figure 10 Previous Rear Toe Link

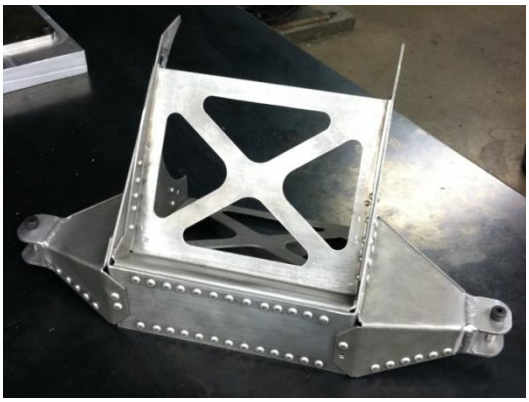

Figure 11 Aluminum Toe Bracket

Figure 12 Welded Section of Toe Bracket

Figure 13 Carbon Fiber A-arms

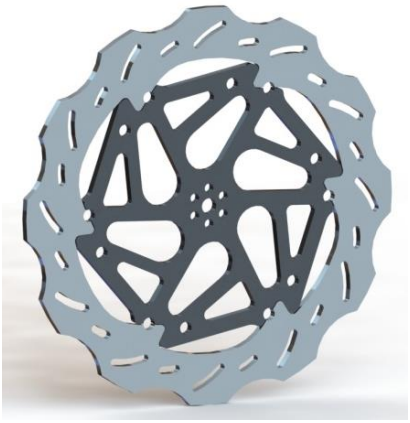

Figure 21 Front Rotors

Figure 17 Diffuser Model

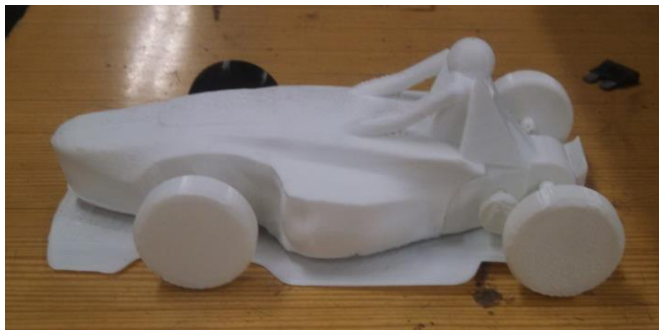

Figure 18 3D Printed Model

Figure 20 Master Cylinder Redesign

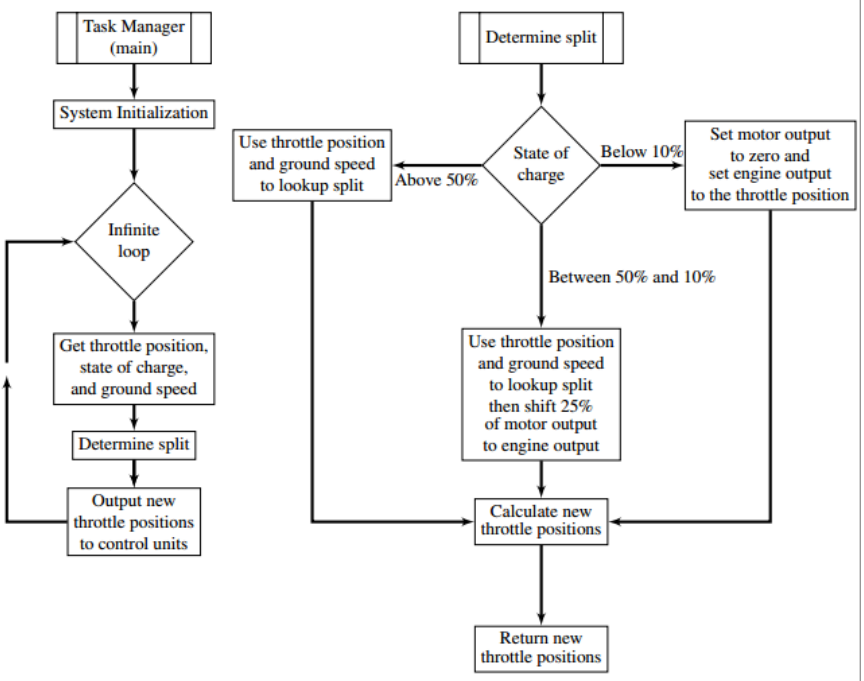

Figure 15 Control System Flow Diagrams

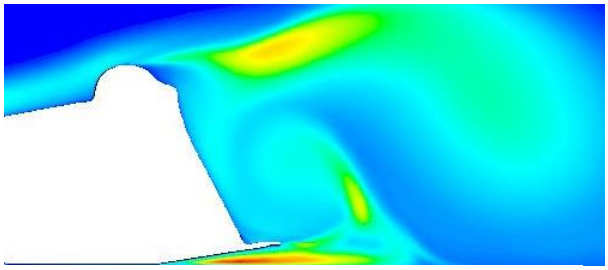

Figure 16 Turbulence Generation for Fixed Rake Diffuser

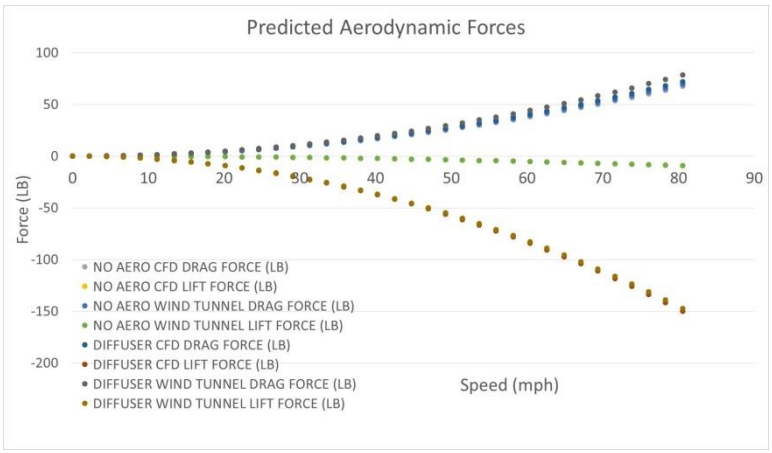

Figure 19 Predicted Aerodynamic Forces

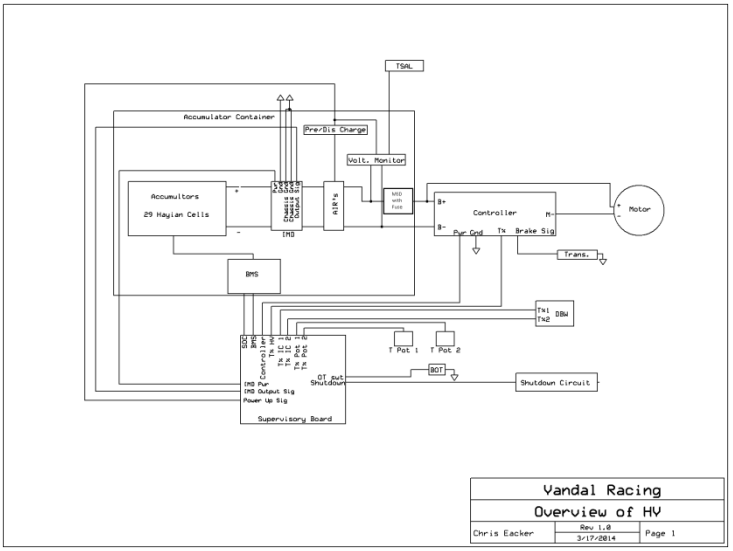

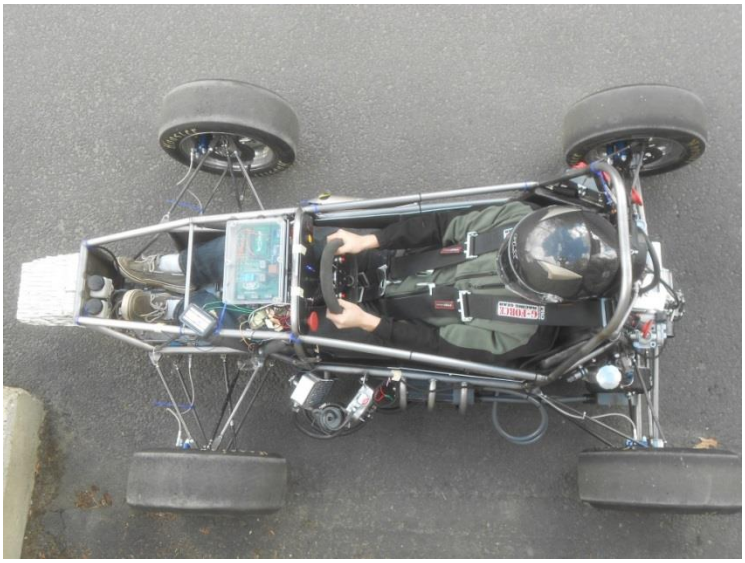

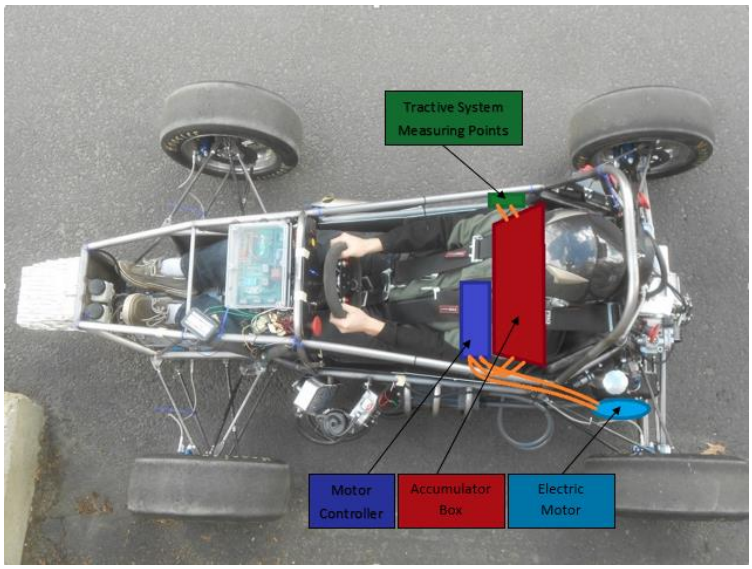

Table 1 Epoxy Bond Strength

Epoxy	Failure Load [lbf]
HP-120	2786
HP-120	1192
HP-120	2561
HP-120	2742
9430	2530
9430	2856
9430	2090
9430	1665

Table 2 Tested Lengths of Inserts (HYSAE-120HP)

Insert Length [inches]	Failure Load [lbf]
.5	1135
.5	2645
.5	2110
.75	2538
.75	2538
.75	2538
1	3475
1	1559
1	2129

Table 3 A-arm Length and Strength

	Front				Rear				
	Upper Forward	Upper Rear	Lower Forward	Lower Rear	Upper Forward	Upper Rear	Lower Forward	Lower Rear	Toe
Tube OD	0.5	0.5	0.6	0.6	0.5	0.5	0.5	0.7	0.5
Tube ID	0.4	0.4	0.4	0.4	0.4	0.4	0.4	0.5	0.4
tube thickness	0.1	0.1	0.1	0.1	0.1	0.1	0.1	0.1	0.1
Insert Length Minimum 1.5FS	0.2	0.3	1.0	1.0	0.4	0.7	0.1	1.6	0.4
Insert Length Recommended	0.8	0.8	1.0	1.0	0.8	0.8	0.8	1.8	0.8
Surface Area Prediction Strength	2241.4	2241.4	2988.5	2988.5	2241.4	2241.4	2241.4	6973.2	2241.4
Adhesive model prediction strength	2659.8	2659.8	2872.0	2872.0	2659.8	2659.8	2659.8	3508.8	2659.8
Rod Force	480.7	561.2	1852.0	1852.0	761.2	1345.0	129.6	4003.0	700.0

Table 4 Fixed Rake Diffuser Lift and Drag Coefficients

	No Diffuser	4 DEG	9 DEG	15 DEG	30 DEG
C_D	0.34	0.338	0.35	0.37	0.38
C_L	-0.015	-0.8	-1.2	-0.6	-0.05

Table 5 B-spline Lift and Drag Coefficients

	Curve 1	Curve 2	Curve 3	Curve 4
C_D	0.325	0.33	0.325	0.38
C_L	-0.7	-1.1	-0.9	-0.92

Table 6 Diffuser Model Testing and Simulation Results

			CD	CL	L/D Ratio	% difference between tunnel and CFD (no aero -CD,CL; diffuser - CD,CL)
NO AERO		CFD	0.36	-0.05	-0.138888889	0
		WIND TUNNEL	0.37	-0.05	-0.135135135	-2.702702703
AERO	DIFFUSER	CFD	0.385	-0.8	-2.077922078	-3.896103896
		WIND TUNNEL	0.4	-0.75	-1.875	6.25

Table 7 Weight Reduction Items

Battery Box	Suspension	Pedals	Rotors	Uprights	Radiator	Firewall	Scatter Shield	Toe Bracket	Steering	Frame
-30 lbs.	-9.7 lbs.	-2.95 lbs.	-2.1 lbs.	-8 lbs.	-0.6 lbs.	-4.6 lbs.	-1 lbs.	+1.2 lbs.	-1.4 lbs.	-2.75 lbs.